

Coulomb gauge Green functions and Gribov copies in $SU(2)$ lattice gauge theory*

Markus Quandt[†]

University of Tübingen

E-mail: quandt@tphys.physik.uni-tuebingen.de

Giuseppe Burgio

University of Tübingen

E-mail: burgio@tphys.physik.uni-tuebingen.de

Songvudhi Chimchinda

University of Tübingen

E-mail: chimchinda@tphys.physik.uni-tuebingen.de

Hugo Reinhardt

University of Tübingen

E-mail: hugo.reinhardt@uni-tuebingen.de

We reconsider the lattice measurement of Green functions in Coulomb gauge, both in $2+1$ and $3+1$ dimensions, using an improved gauge fixing scheme. The influence of Gribov copies is examined and we find clear indications that Green functions are more strongly affected than previously assumed, in particular for low momenta. Qualitatively, our improved lattice results in the infra-red compare more favourably with recent continuum calculations in the Hamiltonian approach.

The XXV International Symposium on Lattice Field Theory

July 30 - August 4 2007

Regensburg, Germany

*Supported by DFG under contract DFG-Re856/6-1,2.

[†]Speaker.

1. Introduction

Yang-Mills theory in the Coulomb gauge has recently drawn a renewed attention, both in the continuum [1, 2] and on the lattice [4, 5, 6]. In the continuum at least, this interest is mostly due to the remarkable fact that Gauß' law can be resolved explicitly in Coulomb gauge, which gives the remaining vector potential \mathbf{A} a very intuitive notion similar to electrodynamics [8]. Recent variational approaches in the Schrödinger picture even support the idea of a *constituent gluon* [1, 2], which is almost non-interacting in the infrared and thus completely determined by its dispersion relation $\omega(\mathbf{p})$, i.e. the (inverse) equal-time gluon propagator $D(\mathbf{p}) = \frac{1}{2}\omega(\mathbf{p})^{-1}$.

The obvious drawback of the Coulomb gauge is that *manifest* Lorentz invariance is lost at intermediate stages; it may only be recovered at the end of the calculation. Perturbatively, this problem is reflected in the (tree-level) propagators of some fundamental fields, which are instantaneous in time so that many loop integrands are independent of the temporal loop momentum component k_0 . Such integrals are notoriously difficult to regulate with conventional techniques, though they are believed to cancel in the full theory [8]. Still, the issue of renormalisation in Coulomb gauge remains cumbersome, even at the one-loop level [9].

Similar problems arise on the lattice as well. While initial studies of the gluon propagator in Coulomb gauge displayed almost perfect scaling [4, 5], recent studies using improved gf. techniques indicate that the quality of gauge fixing has a significant impact on Green functions; in particular, substantial scaling violations may result [6]. The same conclusion has been drawn earlier in Landau gauge, where careful gauge fixing may alter the infrared behaviour of the propagator quantitatively by as much as 20 % [7].

Even more severe discrepancies arise in the comparison of early lattice results with the variational approach mentioned above. While both methods show good agreement in $D = 2 + 1$, their results in $D = 3 + 1$ differ *qualitatively*, both in the infra-red and the ultra-violet:

| | IR | UV |
|----------------|--|--|
| lattice [4, 5] | $D(\mathbf{p}) \rightarrow \text{const}$ | $D(\mathbf{p}) \sim \mathbf{p} ^{-\frac{3}{2}}$ |
| variation [1] | $D(\mathbf{p}) \rightarrow 0$ | $D(\mathbf{p}) \sim \mathbf{p} ^{-1}$ |

All these findings emphasise the need for a thorough corroboration of lattice results in Coulomb gauge, in particular with regard to the quality of gauge fixing. In the present talk, I will present the first results in this program, viz. the equal time gluon propagator in $D = 2 + 1$ and $D = 3 + 1$. Further studies on the ghost propagator and the Coulomb form factor are currently underway and will be presented elsewhere.

The plan of this talk is as follows: In the next section, I will briefly discuss our gf. techniques and demonstrate that they are effective in reducing the Gribov problem which is at the heart of most gf. issues. Section three presents our findings for the gluon propagator. Some of this data is still preliminary, and so is the quantitative analysis, but our results so far imply both scaling violations in the UV and a significant suppression in the IR. The last point improves the qualitative agreement with variational studies, although the quantitative agreement is still unsatisfactory. In the last section, I will conclude with a brief summary and outlook.

2. Gauge fixing techniques

Coulomb gauge on the lattice can be defined as the maximisation of the functional¹

$$F_t[U] \equiv \frac{1}{3V_3} \text{tr} \sum_{\mathbf{x}} \sum_{i=1}^3 \frac{1}{2} \text{tr} U_i(\mathbf{x}, t) \stackrel{!}{=} \max, \quad V_3 \equiv \prod_{i=1}^3 N_i. \quad (2.1)$$

Here, $U_\mu(x)$ are the link variables, the sum over \mathbf{x} runs over all sites in a fixed *time-slice* $t = \text{const}$ and the maximisation is along the gauge orbit, i.e. with respect to all gauge rotations $\Omega(\mathbf{x}, t)$ of the link field $U_\mu(x)$. As indicated, the Coulomb condition $F_t \stackrel{!}{=} \max$ can be implemented at each time-slice t *independently*. This leaves a residual invariance of space-independent but time dependent gauge transformations $\Omega(t)$, i.e. a global gauge rotation in every time slice.

For the equal-time gluon propagator²

$$D(\mathbf{p}) \sim \int d^3\mathbf{x} e^{i\mathbf{p} \cdot (\mathbf{x} - \mathbf{y})} \sum_{i=1}^3 \sum_{c=1}^3 \langle A_i^c(\mathbf{x}, t) A_i^c(\mathbf{y}, t) \rangle = |\mathbf{p}|^{-1} + \mathcal{O}(\hbar) \quad (2.2)$$

the residual gauge fixing is irrelevant and it is sufficient to fix only the time slice in which the measurement is taken. This is no longer true for other correlators such as the $A_0 - A_0$ propagator related to the static Coulomb potential. Moreover, recent perturbative studies [9] indicate that possible scaling violations in $D(\mathbf{p})$ may be attributed to the loss of covariance at equal times; it will then be necessary to consider the full gluon propagator at all (unequal) times, and Coulomb gauge fixing at all time slices must be augmented by a suitable choice for the residual symmetry.

The Gribov problem, which is at the heart of most g.f. issues, can be expressed as the fact that (2.1) has many *local* maxima which may, however, give inequivalent contributions to non-gauge invariant quantities such as the Green functions. Uniqueness can be enforced by searching for the *global* maximum of (2.1), an NP-hard problem. Our strategy to reduce the influence of Gribov copies is to prepend the standard (over)relaxation algorithm by an initial *preconditioning* step combined with multiple *Gribov repetitions* from random starts. This method is a less expensive substitute for full simulated annealing and works well for small to medium size volumina up to $V \approx 36^4$.

2.1 Preconditioning

The periodic boundary conditions on the lattice allow for a somewhat larger symmetry than just the periodic local gauge rotations. This is well-known from the $SU(2)$ lattice center symmetry: In this case, one multiplies all links $U_0(t, \mathbf{x})$ pointing out of a fixed time-slice³ $t = \text{const}$ by (-1) . This construction flips the sign of all Polyakov lines, but it leaves all plaquettes (and thus the action) invariant; it is therefore a genuine symmetry of the system. In Landau gauge, one can generalise this construction to all four directions, giving a total of 2^4 possible combinations of *flips* [7].

¹For simplicity, we work exclusively with the colour group $G = SU(2)$.

²Gauge potentials are extracted from the link variables in the usual fashion via an $\mathcal{O}(a^2)$ improvement of the basic formula $A_\mu = \frac{1}{2a} [U_\mu(x) - U_\mu^\dagger(x)]$.

³The actual location of the time slice t is irrelevant, since a center flip at a different time-slice t' can be decomposed into a flip at t followed by a strictly local, periodic gauge transformation.

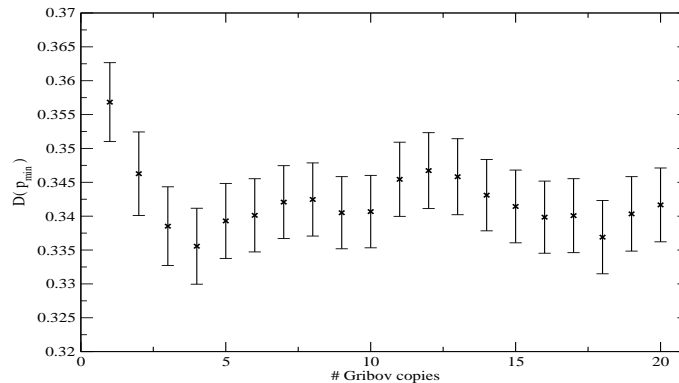


Figure 1: The equal-time gluon propagator at the smallest non-zero lattice momentum, measured as a function of the number N of Gribov repetitions. Data was collected on a 24^4 lattice with $\beta = 2.15$ (left) and $\beta = 2.20$ (right); a total of 200 thermalised configuration were analysed for each data point.

In the Coulomb case, the gauge fixing is carried out in a fixed $3D$ time-slice, i.e. the flips are only carried out in spatial directions, and only the $2D$ sub-planes perpendicular to a given direction (at fixed t) are flipped. The *preconditioning* consist of trying all 2^3 twists to maximise $F_t[U]$ prior to the actual relaxation step. This can be viewed as a non-local update representing a large symmetry transformation that no local relaxation algorithm is likely to find. Flips can also be interspersed at any time during relaxation, although they are most efficient early on, when the algorithm has not yet converged onto a target maximum.⁴

2.2 Multiple Gribov repetitions

The gf. sequence consisting of preconditioning, relaxation and overrelaxation can be repeated multiple times with random starting points. This inspects different regions of the search space and converges to distinct Gribov copies. What makes this repetition effective is that a relatively small number N of copies gives a large increase in the gf. functional, while subsequent repetitions beyond a certain *plateau* point do not give any substantial improvement within reasonable computation time.

This can be seen in figure 1, which plots the equal-time Gluon propagator $D(\mathbf{p})$ at the smallest non-zero lattice momentum, as a function of the number N of Gribov repetitions. The net effect of the improved gauge fixing is generally to suppress $D(\mathbf{p}_{\min})$. Even for N as small as $N = 2, \dots, 5$, the corrections are in the range of 10%. Further copies give smaller corrections; it is then a matter of experiment to find the optimal tradeoff between CPU time and gf. quality. The optimal N will depend quite sensitively on the lattice size and other simulation parameters. In fig. 1 one can see the plateau setting in rather quickly, while our largest lattices ($V = 36^4$) required up to $N = 30$ repetitions.

⁴The (over)relaxation algorithm is iterated until the local gf. violation, i.e. the (maximal norm at all sites \mathbf{x} of the) local gradient of (2.1) is smaller than 10^{-13} .

3. Results

3.1 $D = 2 + 1$

In this case, our findings in fig. 2 are in fair agreement to previous lattice calculations [4, 5]. Our improved gauge fixing scheme has again the tendency to suppress the gluon propagator in the infra-red, but since $D(|\mathbf{p}|) \rightarrow 0$ at small $|\mathbf{p}|$ even without gf. improvment, the *qualitative* behaviour of the gluon propagator is unchanged.

In the UV, we observe scaling in the sense that the various propagator curves for different values of the coupling β can be multiplied by a momentum-independent factor $Z(\beta)$ such that all curves coalesce to a single line. There is a tendency for the scaling to be less perfect than without the gf. improvement, but this is well below the error bars of our numerical simulation.

Quantitatively, the suppression of the gluon propagator in the infra-red is as large as 10% – 15%. To fit the curve in the deep IR and UV region, we have placed two cuts on the data. In the IR, a power ansatz yields

$$D(|\mathbf{p}|) = |\mathbf{p}|^\alpha \cdot (c_1 + c_2 |\mathbf{p}|^2 + \dots), \quad \alpha \approx 0.85(10). \quad (3.1)$$

Since the curve flattens towards the maximum, the exponent α is somewhat depending on the exact location of the IR cut. At $\Lambda = 0.5 \text{ GeV}$, we have $\alpha = 0.81$, while it increases to the above value $\alpha = 0.85$ for $\Lambda = 0.4 \text{ GeV}$. With our present lattice sizes, we cannot go much lower with the IR cut, but the present trend does certainly not rule out the value $\alpha = 1$ preferred by Hamiltonian approaches [1].

In the ultra-violet, a power-law decay

$$D(|\mathbf{p}|) \sim |\mathbf{p}|^{-\gamma}, \quad \gamma \approx 1.5(1) \quad (3.2)$$

is possible, but the exact value of the exponent γ depends quite sensitively on the location of the UV cut. A double-logarithmic plot in the deep UV is *not* a straight line at large momenta, which points to sizeable logarithmic corrections. In fact, an ad-hoc ansatz

$$D(p) \sim \frac{1}{|\mathbf{p}| \cdot \ln |\mathbf{p}|^\delta}$$

with $\delta \approx 0.51$ can fit the data equally well. The conclusion is that our present data does not contain large enough momenta to distinguish between a logarithmic or a power-like behaviour in the UV.

3.2 $D = 3 + 1$

The left panel of fig. 3 shows the results for the largest lattice that we considered. The improved gf. scheme is now seen to make a *qualitative* difference, both in the IR and the UV.

At low momenta, the propagator is clearly *suppressed* as compared to less intricate gf. procedures. The power-law fit explained in the last subsection reveals a IR exponent of

$$\alpha \approx 0.24(12),$$

again with significant variations as the IR cut on the data is changed. However, a value $\alpha = 0$, i.e. a gluon propagator going to a constant as $\mathbf{p} \rightarrow 0$ [4, 5] seems much more unlikely than the vanishing

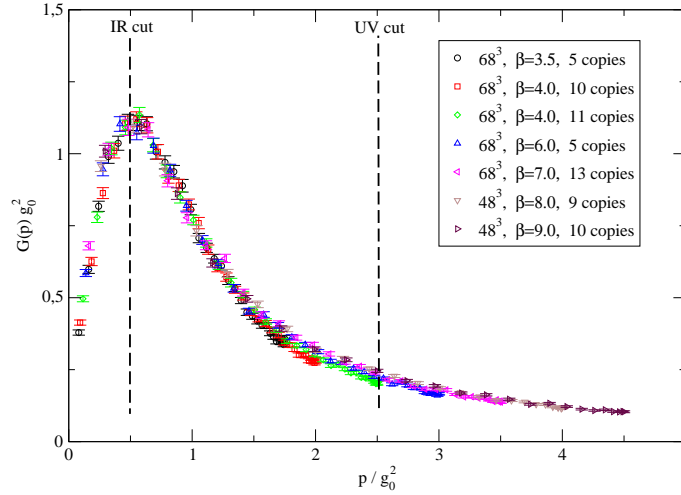


Figure 2: The renormalised equal-time gluon propagator for various couplings and lattice sizes. For the significance of the two data cuts, see the main text.

$D(0) = 0$ predicted by variational calculations [1]. On the other hand, the comparison with the $D = 2 + 1$ case indicates that much smaller momenta must be sampled to rule out one or the other option.

In the UV, the most striking difference to previous lattice results is the absence of perfect scaling, i.e. the gluon propagator does not seem to be multiplicatively renormalisable. This can be clearly seen in the logarithmic plot in the right panel of fig. 3. In a multiplicatively renormalisable situation, we would expect the curves for all couplings β to have the same *slope* at large momenta – which is clearly not the case.

One can now proceed and renormalise anyway such that a common curve can be observed in one p -region or the other (the right panel of fig. 3 has been renormalised to fit well in the IR). In particular, one could try to fit the deep UV region, at the expense of sacrificing a common curve in the IR. From such a fit, it is even possible to extract a power-like behaviour

$$D(\mathbf{p}) \sim |\mathbf{p}|^{-\alpha}, \quad \alpha = 1.57.$$

which is in fair agreement with ref. [4]. Our present data, however, does not warrant such a procedure. In particular, an ad-hoc logarithmic ansatz as in the last subsection would work equally well. To summarize, the scaling violations displayed by our improved gf. scheme are so severe that any attempt to extract a consistent UV behaviour from a multiplicative renormalisation seems ill-advised.

Comparable problems with renormalisation were also found in other studies employing improved gf. schemes. Continuum perturbation theory [9] attributes the scaling violations to the instantaneous nature of the propagator considered here.

4. Summary and conclusions

In this talk, I have presented first results for the equal-time gluon propagator measured in an

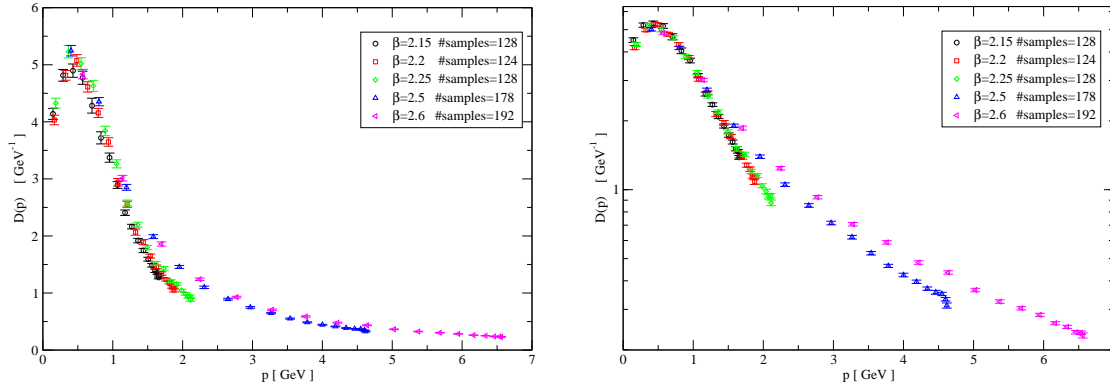


Figure 3: Left panel: The equal-time gluon propagator for various values of the coupling constant. The gauge fixing includes preconditioning and a minimum of 30 Gribov repetitions for each measurement; multiplicative renormalisation focused on the IR data. Right panel: The same data in a logarithmic plot.

improved Coulomb gauge fixing scheme. The general observation is a significant *suppression* of the propagator in the infrared, and a *loss of scaling* at very large momenta. Although the numerics is not fully compelling, the IR data points to $D(0) = 0$ as a likely scenario even for $D = 3 + 1$. The failure of multiplicative renormalisation in the UV has also been observed in other studies treating Coulomb gauge with improved gf. techniques; in perturbation theory, this failure can presumably be attributed to a loss of covariance for the equal-time propagator.

To make the present numbers more convincing, we have to go to smaller momenta, which may involve a simulated annealing step in the gf. pipeline. To get a handle on the scaling issue, it would also be interesting to study the gluon propagator at non-equal times, using a complete gauge fixing that also destroys the residual symmetry in Coulomb gauge. Further investigations involve the ghost propagator and the Coulomb form factor, which are of immediate relevance for the physics of the gauge system. These studies are currently underway and will be presented elsewhere.

References

- [1] C. Feuchter and H. Reinhardt, Phys. Rev. **D70** (2004) 105021;
H. Reinhardt and C. Feuchter, Phys. Rev. **D71** (2005) 105002.
- [2] A.P. Szczepaniak and E.S. Swansen, Phys. Rev. **D65** (2002) 025015.
- [3] D. Eppe, H. Reinhardt and W. Schleifenbaum, Phys. Rev. **D75** (2007) 045011;
H. Reinhardt, W. Schleifenbaum, D. Eppe, C. Feuchter, arXiv:0710.0316 [hep-th]
- [4] K. Landfeld and L. Moyaerts, Phys. Rev. **D70** (2004) 074507.
- [5] A. Cucchieri and D. Zwanziger, Phys. Rev. **D65** (2002) 014001.
- [6] A. Voigt et. al. , arXiv:0709.4585 [hep-lat]
- [7] I.L. Bogolubsky et. al. , Phys. Rev. **D74** (2006) 034503.
- [8] D. Zwanziger, Nucl. Phys. **B518** (1998) 237.
- [9] P. Watson and H. Reinhardt, arXiv:0709.0140 [hep-th].